Human Molecular Genetics, 2014, Vol. 23, No. 19 **5052–5060**
doi:10.1093/hmg/ddu217
Advance Access published on May 12, 2014

Impaired degradation of WNK1 and WNK4 kinases causes PHAII in mutant KLHL3 knock-in mice

Koichiro Susa[1,†], Eisei Sohara[1,†,*], Tatemitsu Rai[1], Moko Zeniya[1], Yutaro Mori[1], Takayasu Mori[1], Motoko Chiga[1], Naohiro Nomura[1], Hidenori Nishida[1], Daiei Takahashi[1], Kiyoshi Isobe[1], Yuichi Inoue[1], Kenta Takeishi[1], Naoki Takeda[2], Sei Sasaki[1] and Shinichi Uchida[1]

[1]Department of Nephrology, Graduate School of Medical and Dental Sciences, Tokyo Medical and Dental University, 1-5-45 Yushima Bunkyo, Tokyo 113-8519, Japan and [2]Division of Transgenic Technology, Institute of Resource Development and Analysis, Kumamoto University, 2-2-1 Honjo Chuo Kumamoto, Kumamoto 860-0811, Japan

Received February 25, 2014; Revised April 19, 2014; Accepted May 5, 2014

Pseudohypoaldosteronism type II (PHAII) is a hereditary disease characterized by salt-sensitive hypertension, hyperkalemia and metabolic acidosis, and genes encoding with-no-lysine kinase 1 (WNK1) and WNK4 kinases are known to be responsible. Recently, Kelch-like 3 (KLHL3) and Cullin3, components of KLHL3-Cullin3 E3 ligase, were newly identified as responsible for PHAII. We have reported that WNK4 is the substrate of KLHL3-Cullin3 E3 ligase-mediated ubiquitination. However, WNK1 and Na–Cl cotransporter (NCC) were also reported to be a substrate of KLHL3-Cullin3 E3 ligase by other groups. Therefore, it remains unclear which molecule is the target(s) of KLHL3. To investigate the pathogenesis of PHAII caused by KLHL3 mutation, we generated and analyzed KLHL3$^{R528H/+}$ knock-in mice. KLHL3$^{R528H/+}$ knock-in mice exhibited salt-sensitive hypertension, hyperkalemia and metabolic acidosis. Moreover, the phosphorylation of NCC was increased in the KLHL3$^{R528H/+}$ mouse kidney, indicating that the KLHL3$^{R528H/+}$ knock-in mouse is an ideal mouse model of PHAII. Interestingly, the protein expression of both WNK1 and WNK4 was significantly increased in the KLHL3$^{R528H/+}$ mouse kidney, confirming that increases in these WNK kinases activated the WNK-OSR1/SPAK-NCC phosphorylation cascade in KLHL3$^{R528H/+}$ knock-in mice. To examine whether mutant KLHL3 R528H can interact with WNK kinases, we measured the binding of TAMRA-labeled WNK1 and WNK4 peptides to full-length KLHL3 using fluorescence correlation spectroscopy, and found that neither WNK1 nor WNK4 bound to mutant KLHL3 R528H. Thus, we found that increased protein expression levels of WNK1 and WNK4 kinases cause PHAII by KLHL3 R528H mutation due to impaired KLHL3-Cullin3-mediated ubiquitination.

INTRODUCTION

Pseudohypoaldosteronism type II (PHAII) is a hereditary disease characterized by salt-sensitive hypertension, hyperkalemia, and metabolic acidosis (1,2). Mutations in with-no-lysine kinase 1 (WNK1) and WNK4 genes were reported to be responsible for PHAII (3). It was previously demonstrated that the WNK kinase family phosphorylates and activates oxidative stress-responsive kinase 1 (OSR1) and STE20/ SPS1-related proline/alanine-rich kinase (SPAK) (4,5), and that activated OSR1/SPAK kinases could phosphorylate and activate Na–Cl cotransporter (NCC), constituting the WNK-OSR1/SPAK-NCC phosphorylation signaling cascade. This regulation of NCC by WNK-OSR1/SPAK signaling was confirmed *in vivo* using various genetically engineered mouse models (6–14). Through analysis of the WNK4 knock-in PHAII mouse model, constitutive activation of this WNK-OSR1/SPAK-NCC phosphorylation cascade in kidney was found to be the major pathogenic mechanism of PHAII.

Recently, two additional novel genes, Kelch-like 3 (KLHL3) and Cullin3, were identified as responsible for PHAII (15,16). KLHL3 is a member of the BTB–BACK–Kelch family, which are known as substrate adapters of Cullin3-based E3 ubiquitin ligase complexes (17–20). We and others have reported

*To whom correspondence should be addressed at: Eisei Sohara, Department of Nephrology, Graduate School of Medical and Dental Sciences, Tokyo Medical and Dental University, 1-5-45 Yushima Bunkyo, Tokyo 113-8519, Japan. Tel: +81-3-5803-5214; Fax: +81-3-5803-5215; Email: esohara.kid@tmd.ac.jp
††These authors contributed equally to this work.

that KLHL3 interacts with Cullin3 and WNK4, induces WNK4 ubiquitination and reduces WNK4 protein levels in cultured cells and *Xenopus laevis* oocytes (21–24). Interestingly, it was also reported that WNK1 could be a substrate of KLHL3-Cullin3 E3 ubiquitin ligase (21,24). Moreover, another group reported that KLHL3 was able to bind to NCC and regulate its intracellular localization in cultured cells (16). Therefore, it remains unclear which molecule involved in the pathogenesis of PHAII is the *in vivo* target of KLHL3. In addition, the above experiments were performed in cultured cells. Thus, it is necessary to clarify the role of KLHL3 mutation in PHAII pathogenesis *in vivo*.

In this study, to answer these questions, we generated KLHL3$^{R528H/+}$ knock-in mice that carry the same mutation as autosomal dominant type PHAII patients. This KLHL3$^{R528H/+}$ knock-in PHAII model mouse revealed that increased protein expression levels of WNK1 and WNK4 kinases, due to impaired binding of KLHL3 with WNK kinases, cause PHAII *in vivo*. These results also indicated that both WNK1 and WNK4 are physiologically regulated by KLHL3-Cullin3-mediated ubiquitination *in vivo*.

RESULTS

Generation of KLHL3$^{R528H/+}$ knock-in mice

KLHL3$^{R528H/+}$ knock-in mice were generated using homologous recombination in Baltha1 embryonic stem (ES) cells to create a mutant allele (25). Exon 15 of the Klhl3 gene was replaced by a cassette expressing a neomycin selective marker flanked by loxP sites, which was followed by the mutant exon 15 (R528H) (Fig. 1A). Recombinant ES cell clones were injected into morula to generate chimeric mice. The neo cassette was deleted by crossing the mutant KLHL3$^{flox/+}$ mice with CAG promoter-Cre transgenic mice. Successful generation of KLHL3$^{R528H/+}$ knock-in mice was confirmed by genomic sequencing (Fig. 1B–E). In addition to the generation of KLHL3$^{R528H/+}$ heterozygous mice, we generated KLHL3$^{R528H/R528H}$ homozygous mice to more readily detect the pathological effects of mutant KLHL3 R528H.

PHAII phenotypes of KLHL3$^{R528H/+}$ knock-in mice

There were no significant differences in body weight and physical appearance between KLHL3$^{R528H/+}$ and wild-type mice. To confirm the KLHL3$^{R528H/+}$ mouse as an accurate model of PHAII, we measured systolic blood pressure of mice fed a normal-salt diet. The systolic blood pressure in the KLHL3$^{R528H/+}$ mice fed a normal-salt diet did not differ from that of wild-type mice (Table 1). Since PHAII shows salt-sensitive hypertension, we then measured blood pressure in mice fed a high-salt diet, which revealed that a high-salt diet produced significantly higher systolic blood pressure in KLHL3$^{R528H/+}$ mice compared with wild-type mice (133.5 ± 1.6 mmHg versus 120.1 ± 5.1 mmHg, respectively; $n = 5$ and 4, $P < 0.05$). Moreover, as shown in Table 2, KLHL3$^{R528H/+}$ mice exhibited hyperkalemia and metabolic acidosis similar to PHAII patients. These data clearly indicate that the KLHL3$^{R528H/+}$ mouse is an ideal model of PHAII caused by KLHL3 mutation. The severity of hyperkalemia and metabolic acidosis was not changed under a high-salt diet (Supplementary Material, Fig. S1). We also performed blood pressure measurement and analysis of blood biochemical characteristics of KLHL3$^{R528H/R528H}$ homozygous knock-in mice (Tables 1 and 2). Although KLHL3$^{R528H/R528H}$ mice also exhibited salt-sensitive hypertension, hyperkalemia and metabolic acidosis, the blood pressure and blood biochemistries did not significantly differ from those of KLHL3$^{R528H/+}$ mice.

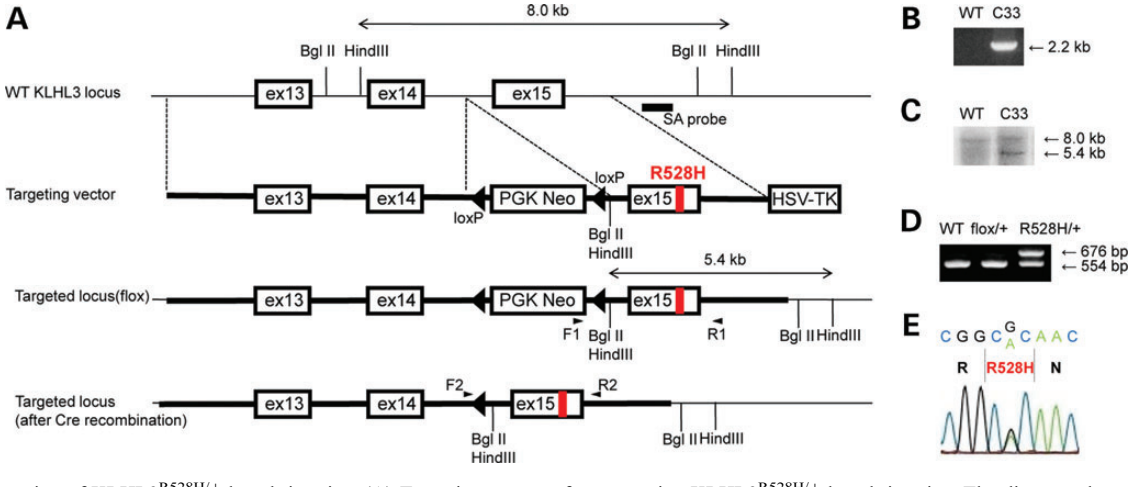

Figure 1. Generation of KLHL3$^{R528H/+}$ knock-in mice. (**A**) Targeting strategy for generating KLHL3$^{R528H/+}$ knock-in mice. The diagram shows the wild-type KLHL3 locus, the targeting construct and the targeted locus before and after Cre recombination. (**B**) Verification of homologous recombination by PCR of genomic DNA of the selected ES cell clones; primers F1 and R1 were as shown in (A). The 2.2 kb band is from the mutated allele. The primer set was designed to prevent amplification of the wild-type KLHL3 gene. C33 is the name of the selected ES cell clone. WT, host ES cells. (**C**) Verification of homologous recombination by Southern blotting of Hind III-digested genomic DNA derived from mouse tails. The 8.0 kb band is from the wild-type allele and the 5.4 kb band is from the mutated allele. (**D**) Genotyping PCR after Cre recombination using a primer set (F2 and R2) flanking the remaining loxP site. The 676 bp band represents the mutant allele containing the remaining loxP site, while the 554 bp band represents the wild-type allele. WT, wild-type mice; flox/+, KLHL3$^{flox/+}$ (R528H) mice; R528H/+, KLHL3$^{R528/+}$ mice. (**E**) Direct sequencing of the PCR product covering the mutation site.

Table 1. Blood pressure of wild-type, KLHL3$^{R528H/+}$, and KLHL3$^{R528H/R528H}$ mice

	WT	KLHL3$^{R528H/+}$	KLHL3$^{R528H/R528H}$
Systolic blood pressure (mmHg)			
Under normal diet	122.5 ± 2.0 ($n = 7$)	125.3 ± 3.0 ($n = 7$)	124.2 ± 1.6 ($n = 4$)
Under high-salt diet	120.1 ± 5.1 ($n = 4$)	133.5 ± 1.6* ($n = 5$)	136.3 ± 2.0* ($n = 4$)

*$P < 0.05$ compared with wild-type mice. No significant difference between KLHL$^{R528H/+}$ and KLHL3$^{R528H/R528H}$ mice was observed.

Table 2. Blood biochemical characteristics of wild-type, KLHL3$^{R528H/+}$, and KLHL3$^{R528H/R528H}$ mice

	WT	KLHL3$^{R528H/+}$	KLHL3$^{R528H/R528H}$
Blood biochemistries			
Na^+ (mmol/l)	149.0 ± 0.4	149.7 ± 0.4	149.9 ± 1.0
K^+ (mmol/l)	4.1 ± 0.1	4.8 ± 0.1*	4.8 ± 0.3*
Cl^- (mmol/l)	113.1 ± 0.4	116.0 ± 0.6*	115.8 ± 1.0*
BUN (mg/dl)	24.1 ± 1.4	22.9 ± 0.9	27.5 ± 2.4
Glu (mg/dl)	221.8 ± 8.3	219.3 ± 11.4	192.3 ± 17.9
pH	7.321 ± 0.008	7.287 ± 0.011*	7.261 ± 0.025*
pCO_2 (mmHg)	44.5 ± 1.4	46.1 ± 1.6	47.1 ± 3.1
$HCO3^-$ (mmol/l)	23.5 ± 0.4	21.7 ± 0.4*	20.7 ± 0.4*
Hb (g/dl)	14.7 ± 0.3 ($n = 12$)	14.6 ± 0.2 ($n = 12$)	14.5 ± 0.3 ($n = 8$)

BUN, blood urea nitrogen; Glu, glucose; Hb, hemoglobin. No significant difference between KLHL$^{R528H/+}$ and KLHL3$^{R528H/R528H}$ mice was observed in any values.
*$P < 0.05$ compared with wild-type mice.

Increased protein expression levels of WNK1 and WNK4 in KLHL3$^{R528H/+}$ mouse kidney

To investigate the pathogenesis of PHAII caused by the R528H mutation of KLHL3 *in vivo*, we examined the protein expression and phosphorylation of molecules constituting the WNK signaling pathway. As shown in Figure 2A and B, protein expression levels of WNK1 and WNK4 were significantly increased 1.8- and 1.4-fold, respectively, in the kidney of KLHL3$^{R528H/+}$ mice compared with those of wild-type mice. Accordingly, phosphorylation of OSR1, SPAK and NCC was also increased in KLHL3$^{R528H/+}$ mice. The KLHL3$^{R528H/R528H}$ homozygous mouse showed obvious increases of WNK1 and WNK4 protein levels (6.9- and 2.4-fold, respectively, compared with wild-type mice) and increased phosphorylation of OSR1 and SPAK. However, we also found that the protein level and the phosphorylation status of NCC in KLHL3$^{R528H/R528H}$ homozygous knock-in mice were not significantly increased compared with those in KLHL3$^{R528H/+}$ heterozygous knock-in mice, suggesting that the levels of increased WNK1 and WNK4 in the KLHL3$^{R528H/+}$ heterozygous knock-in mice might be high enough to fully phosphorylate and activate NCC. Considering that constitutive activation of NCC is the cause of PHAII, this saturated phosphorylation status of NCC could explain why the blood pressure and blood chemistries in KLHL3$^{R528H/R528H}$ homozygous knock-in mice did not differ from those of KLHL3$^{R528H/+}$ mice (Tables 1 and 2).

In addition, we confirmed that mRNA levels of WNK1 and WNK4 were not increased in the KLHL3$^{R528H/+}$ heterozygous mouse kidney (Fig. 2C), indicating that the increased protein levels of WNK1 and WNK4 were due to impaired degradation rather than transcriptional activation. To confirm that protein expression levels of WNK1 and WNK4 were increased in distal convoluted tubules (DCTs) where NCC is present, we performed double immunofluorescence of mouse kidney. As shown in Figure 3A and B, most of the KLHL3, WNK1 and WNK4 signals were colocalized with NCC, and signal intensities of WNK1 and WNK4 at DCT were apparently higher in the KLHL3$^{R528H/+}$ mouse kidney. Considering that both the WNK1 and WNK4 transgenic mice were reported to cause activation of the WNK-OSR1/SPAK-NCC phosphorylation cascade (9,21), these data clearly indicated that the essential pathogenesis of PHAII caused by KLHL3 mutation is due to increased WNK1 and WNK4 in DCT, leading to activation of the WNK-OSR1/SPAK-NCC phosphorylation signaling cascade.

Defective binding between the acidic motif of WNK1/WNK4 and mutant KLHL3 R528H

We had previously reported that KLHL3 mutation in the Kelch domain decreased its binding to the acidic domain of WNK4, leading to impaired ubiquitination and reduced WNK4 protein levels in HEK 293 cells (21). To confirm that the increased protein levels of WNK1 and WNK4 in KLHL3$^{R528H/+}$ mouse kidney were caused by impaired binding between WNK kinases and the mutant KLHL3 R528H, we measured the diffusion time of the TAMRA-labeled acidic motif of WNK1 or WNK4 peptide using fluorescence correlation spectroscopy (FCS) in the presence of different concentrations of GST-fusion proteins of wild-type and mutant KLHL3 R528H; the binding of KLHL3 to these peptides is observed as increased diffusion time of the fluorescent peptide (21,26,27). Wild-type KLHL3 increased the diffusion time of the TAMRA-labeled WNK1 and WNK4 peptides, confirming that wild-type KLHL3 can interact with the acidic motif of WNK1 as well as that of WNK4 (Fig. 4). On the

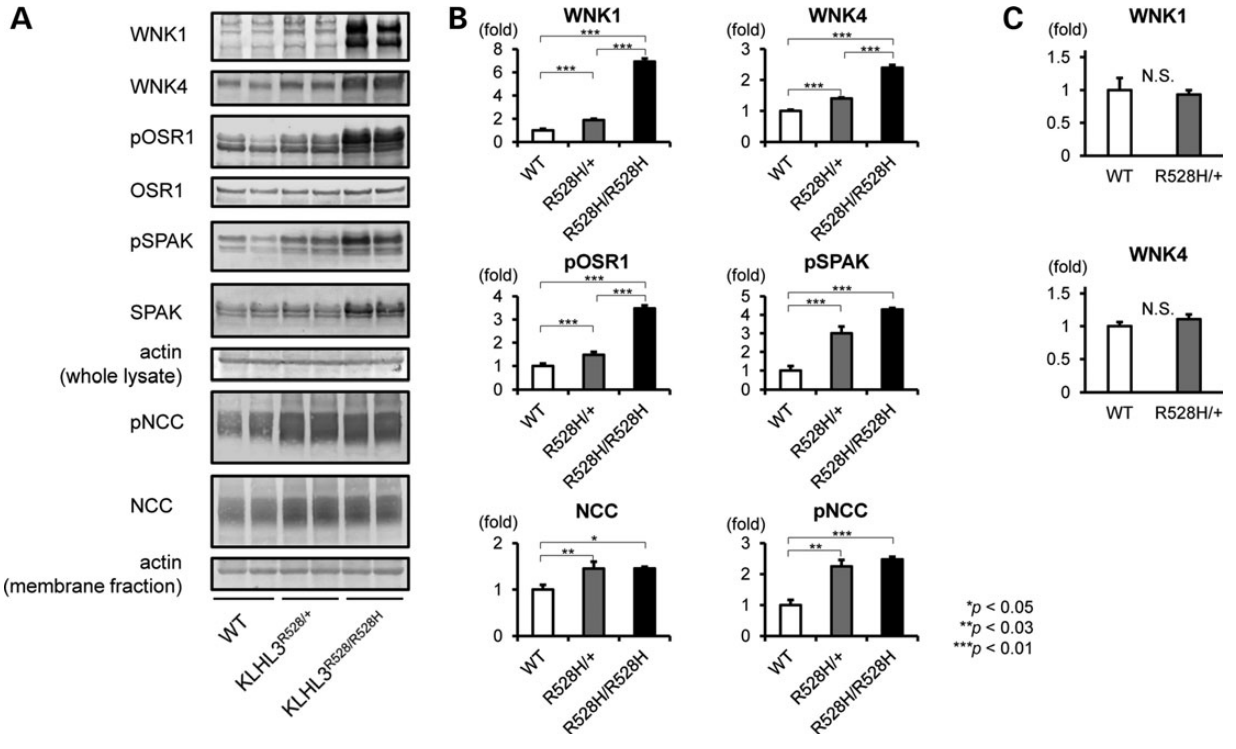

Figure 2. Increased WNK1 and WNK4 protein levels and activation of the WNK-OSR1/SPAK-NCC phosphorylation signaling cascade in KLHL3 mutant mouse kidney. (**A**) Representative immunoblots of the WNK-OSR1/SPAK-NCC signaling cascade in the kidneys of wild-type mice (WT), KLHL3$^{R528H/+}$ heterozygous knock-in mice and KLHL3$^{R528H/R528H}$ homozygous knock-in mice. (**B**) Densitometry analysis; values are expressed as a ratio of the average signal in wild-type mice. KLHL3$^{R528H/+}$ heterozygous knock-in mice and KLHL3$^{R528H/R528H}$ homozygous knock-in mice showed significantly increased protein levels of WNK1 and WNK4. The mutant KLHL3 mice also showed increased phosphorylation of OSR1, SPAK and NCC. WT, wild-type mice; R528H/+, KLHL3$^{R528/+}$ mice; R528H/R528H, KLHL3$^{R528/R528H}$ mice. $n = 6$ to 9. $^{*}P < 0.05$. $^{**}P < 0.03$. $^{***}P < 0.01$. (**C**) Quantitative PCR analysis of WNK1 and WNK4 mRNA levels. SYBR Green quantitative PCR was used to quantify mRNA levels in the kidneys of wild-type mice and KLHL3$^{R528H/+}$ mice. KLHL3$^{R528H/+}$ mice did not show significant differences of WNK1 and WNK4 mRNA levels in the kidney. WT, wild-type mice; R528H/+, KLHL3$^{R528/+}$ mice. $n = 5$.

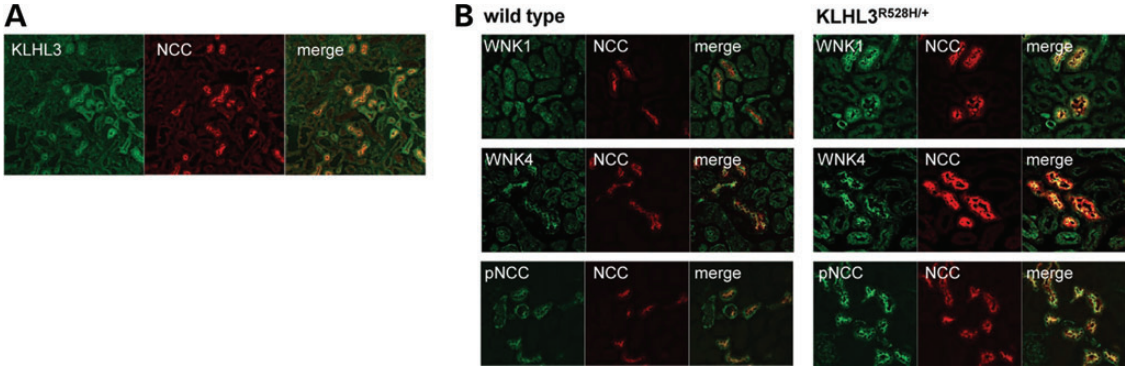

Figure 3. Immunofluorescence of WNK1, WNK4 and NCC in the kidney cortex. (**A**) Double immunofluorescence of KLHL3 and NCC in the kidney cortex of wild-type mice. The KLHL3 signal is colocalized with NCC. (**B**) Double immunofluorescence of WNK1 and NCC (upper), WNK4 and NCC (middle), and phosphorylated NCC and NCC (lower) in the kidney cortex of wild-type mice (left) and KLHL3$^{R528H/+}$ mice (right). Signals of WNK1, WNK4, NCC and pNCC are increased in KLHL3$^{R528H/+}$ mice.

other hand, the diffusion time of TAMRA-labeled WNK1 and WNK4 peptides was not affected by the addition of mutant KLHL3 R528H protein, indicating that neither WNK1 nor WNK4 bind to mutant KLHL3 R528H. The defective binding between WNK kinases and mutant KLHL3 R528H could result in impaired KLHL3-Cullin3 mediated ubiquitination of WNKs, as we previously reported, leading to increased protein expression of WNK kinases and activation of WNK signaling in the KLHL3$^{R528H/+}$ mouse kidney.

Regulation of epithelial Na^+ channels and ROMK in KLHL3$^{R528H/+}$ mice

We investigated epithelial Na^+ channels (ENaC) and renal outer medullary K^+ channels (ROMK), two important channels for Na^+ reabsorption and K^+ secretion in cortical collecting ducts (CCD), in KLHL3$^{R528H/+}$ mice. As shown in Figure 5, although KLHL3$^{R528H/+}$ mice did not show a significant change in the protein levels of total ENaC α subunit (85 kDa) compared

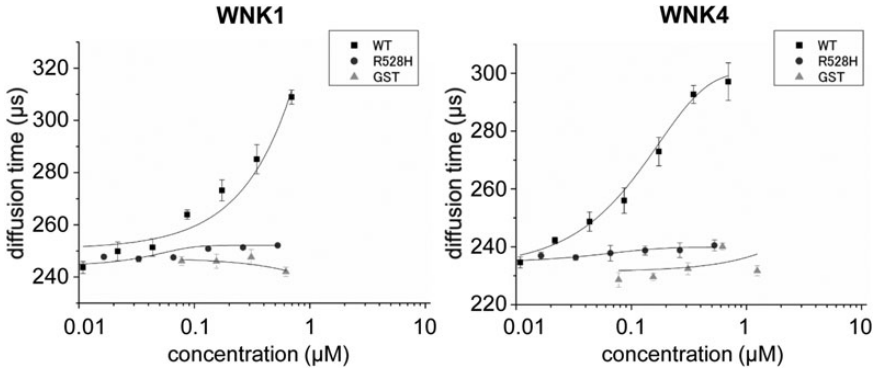

Figure 4. FCS assay of the binding between wild-type/mutant KLHL3 and WNK1/WNK4. The diffusion time of TAMRA-labeled WNK1 and WNK4 peptides containing the acidic motif was measured using FCS in the presence of different concentrations of GST fusion proteins of the wild-type KLHL3 and KLHL3 R528H mutant. The acidic motif of both WNK1 and WNK4 bound to the wild-type GST-KLHL3. On the other hand, GST alone and the KLHL3 R528H mutant did not affect the diffusion time, indicating that the KLHL3 R528H mutant could not bind to the acidic motif of WNK1 and WNK4.

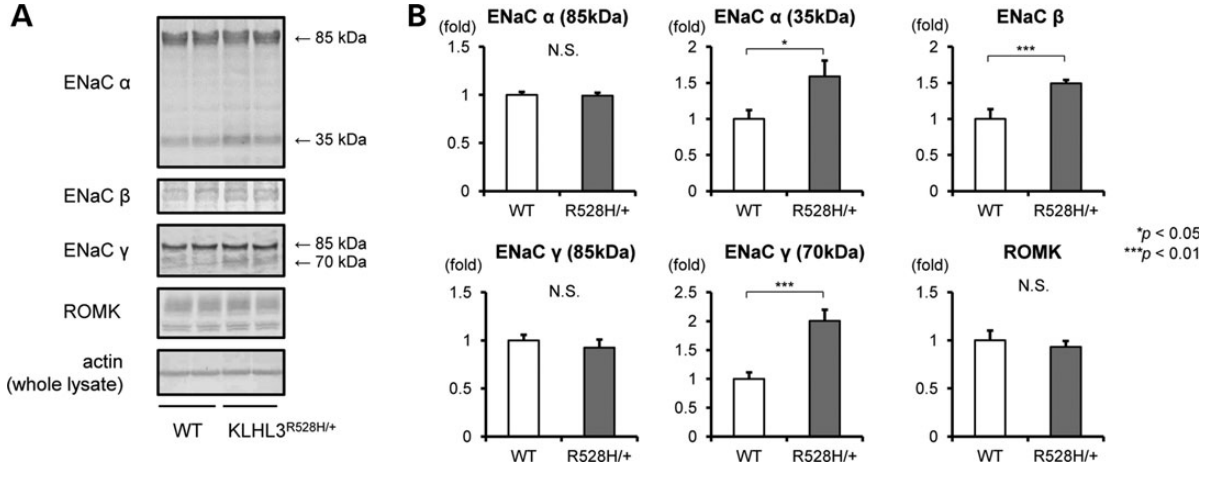

Figure 5. ENaC and ROMK in KLHL3$^{R528H/+}$ mice. (**A**) Representative immunoblots of ENaC α, ENaC β, ENaC γ subunits and ROMK in the kidneys of wild-type mice and KLHL3$^{R528H/+}$ mice. (**B**) Densitometry analysis of ENaC α, ENaC β, ENaC γ subunits and ROMK in the kidneys; values are expressed as a ratio of the average signal in wild-type mice. WT, wild-type mice; R528H/+, KLHL3$^{R528/+}$ mice. $n = 6$ to 9. $^{*}P < 0.05$. $^{***}P < 0.01$.

with wild-type mice, the levels of cleaved ENaC α subunit (35 kDa) were increased in KLHL3$^{R528H/+}$ mice. The level of ENaC β subunit was also increased in KLHL3$^{R528H/+}$ mice. Similar to ENaC α subunit, KLHL3$^{R528H/+}$ mice showed no significant change in the total protein level of ENaC γ subunit (85 kDa). However, a significant increase of cleaved ENaC γ subunit (70 kDa) was found in the KLHL3$^{R528H/+}$ mouse kidney. Similar to WNK4$^{D561A/+}$ knock-in mice (7), these results indicate that ENaC is activated in the KLHL3$^{R528H/+}$ mouse kidney. On the other hand, KLHL3$^{R528H/+}$ mice did not show a significant difference in protein levels of ROMK in immunoblot analysis of whole kidney (Fig. 5).

DISCUSSION

Investigation of the pathophysiology of PHAII is extremely important, not only to increase knowledge of this rare inherited disease, but also for the discovery of novel mechanisms of salt handling in the kidney. Although KLHL3 was identified as responsible for PHAII, several molecules have recently been reported as substrates that interact with KLHL3 in cultured cells. It was demonstrated that the loss of interaction between KLHL3 and WNK4 induced impaired ubiquitination of WNK4 and increased protein levels of WNK4 (21–24). In addition, WNK1 was also reported to be bound to KLHL3 (21,24). In contrast, Louis-Dit-Picard *et al.* (16) reported that KLHL3 is responsible for direct regulation of NCC membrane expression. Therefore, the pathophysiological role of KLHL3 in PHAII required investigation of *in vivo* kidney. For this purpose, we generated KLHL3$^{R528H/+}$ knock-in mice that carry a mutation found in human PHAII patients (15,16). This KLHL3$^{R528H/+}$ knock-in mouse exhibited salt-sensitive hypertension, hyperkalemia and metabolic acidosis, which are characteristic symptoms of PHAII patients. Moreover, increased NCC phosphorylation was also observed. These results clearly confirmed that our KLHL3$^{R528H/+}$ mouse is an ideal model of mutant KLHL3-induced PHAII.

To investigate the mechanisms of PHAII in KLHL3$^{R528H/+}$ mice, we assessed the protein levels and phosphorylation status of the WNK-OSR1/SPAK-NCC phosphorylation signaling cascade. Interestingly, KLHL3$^{R528H/+}$ heterozygous mice showed increased protein levels of both WNK1 and WNK4 in the kidney, and KLHL3$^{R528H/R528H}$ homozygous mice more

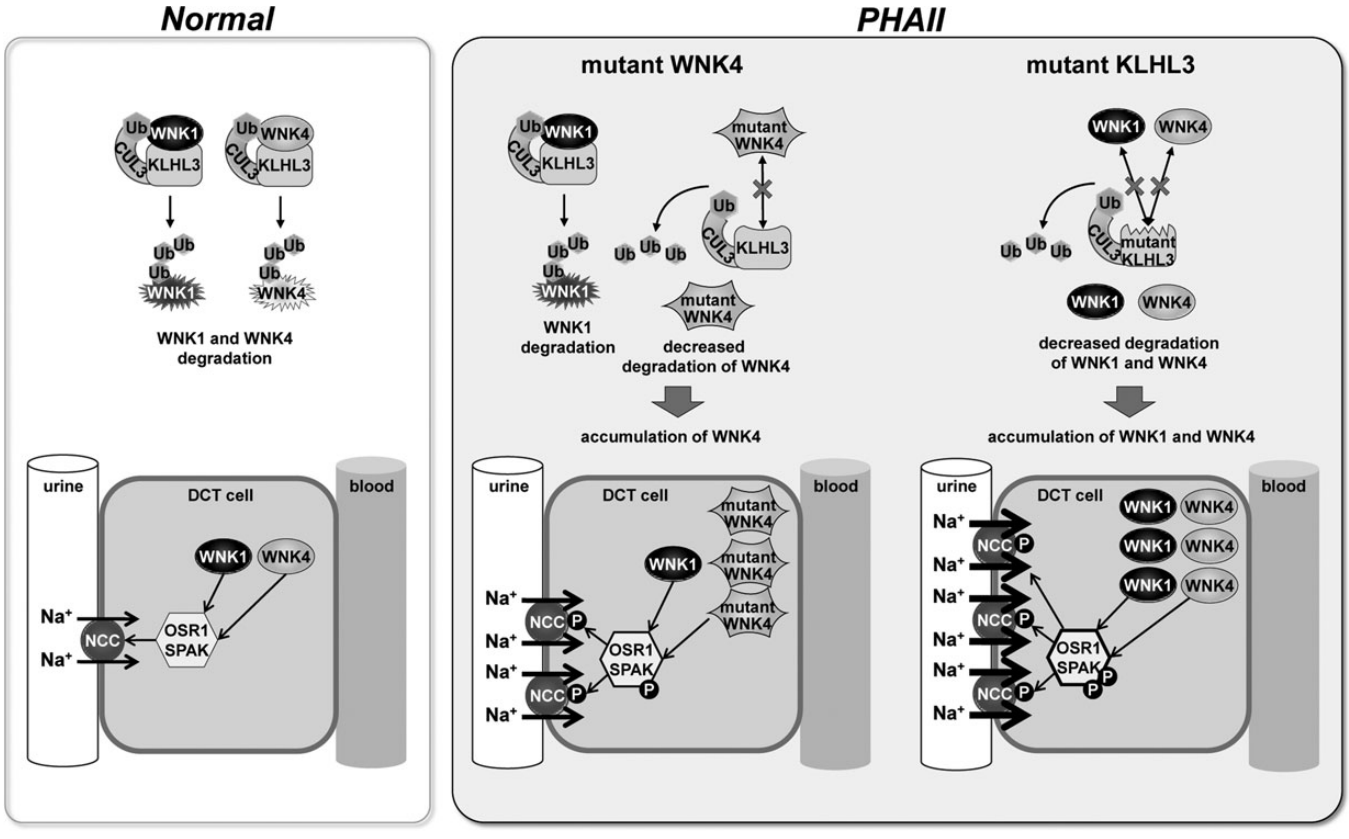

Figure 6. Schematic representation of the mechanism of PHAII caused by KLHL3 mutation.

clearly demonstrated increased WNK1 and WNK4 protein levels. We further demonstrated using an immunofluorescence assay that protein levels of both WNK1 and WNK4 are increased in DCT in KLHL3$^{R528H/+}$ mice. We also confirmed by FCS assay that mutant KLHL3 R528H did not bind to the acidic motif of either WNK1 or WNK4. Considering these observations, we have demonstrated for the first time that the essential mechanism of mutant KLHL3-induced PHAII involves impaired ubiquitination and increased protein levels of both of WNK1 and WNK4 in DCT *in vivo* (Fig. 6).

Importantly, these facts suggest that Cullin3-KLHL3 E3 ligase complexes physiologically regulate WNK-OSR1/SPAK-NCC phosphorylation cascades *in vivo*, indicating that KLHL3 plays an important role in the physiological mechanisms of sodium handling in the kidney. To date, physiological regulators of the WNK-OSR1/SPAK-NCC phosphorylation signal cascade, such as insulin (28–31), angiotensin II (10,32–34) and aldosterone (32,35–37), have been reported. However, the regulatory mechanism of these factors in WNK signaling remains unknown. The novel KLHL3-mediated regulation of WNK signals might be involved in these mechanisms. Further investigation is required to clarify this issue.

It was reported that KLHL3 was able to bind to NCC and regulate its intracellular localization in cultured cells (16). However, WNK and OSR1/SPAK were activated in KLHL3$^{R528H/+}$ mice, but were not down-regulated by increased NCC phosphorylation. Moreover, it was reported that simple over-expression of NCC did not produce the PHAII phenotype in NCC transgenic mice (38), indicating that increased phosphorylation, but not increased protein expression, of NCC is required for the PHAII phenotype *in vivo*. Considering these *in vivo* observations, the essential pathogenesis of PHAII caused by KLHL3 mutation is not due to impaired ubiquitination or regulation of NCC, but to the impaired ubiquitination of WNK kinases. This discrepancy could be due to the experimental system, the genetically engineered mouse model or cultured cells.

Boyden *et al*. (15) reported that symptoms of human PHAII patients caused by KLHL3 mutation are more severe than those caused by mutation in WNK1 or WNK4. WNK4$^{D561A/+}$ knock-in (7) and WNK1$^{+/FHHt}$ (9) PHAII mouse models exhibited increases of only a single kind of WNK kinase that carries a mutation. The increased severity of KLHL3 mutation-induced PHAII in human patients may be explained by the physiological difference between the increase of 'both WNK1 and WNK4 kinases' and 'a single WNK kinase'. Accumulation of both WNK1 and WNK4 kinases by KLHL3 mutation could result in further increases in phosphorylation of downstream components compared with the accumulation of a single WNK kinase (Fig. 6). However, the KLHL3$^{R528H/+}$ mouse shows a less severe phenotype than other mouse models of PHAII previously reported (7,9), which could be explained by the difference of origin of ES cells used for the generation of the knock-in mice, i.e. the difference of genetic background of these mice. In this study we utilized Baltha1 ES cells derived from C57BL/6 mouse, which is a one-renin-gene mouse strain. However, the other mouse models of PHA II were established with ES cells

derived from two-renin-gene mouse strains, 129Sv (7,9). It was reported that 129Sv mice showed increased blood pressure response to salt intake, compared with C57BL/6 mice (39). Further investigation to compare the phenotypes of three PHAII model mice under the same genetic background will be required.

Finally, we discuss the involvement of ENaC and ROMK in PHAII caused by KLHL3 mutation. ENaC was activated in KLHL3$^{R528H/+}$ heterozygous knock-in mice, similar to WNK4$^{D561A/+}$ mice (7). However, inconsistent with the KLHL3$^{R528H/+}$ and WNK4$^{D561A/+}$ mice, WNK1$^{+/FHHt}$ mice are reported to show no activation of ENaC (9). This difference might be explained by whether WNK4 is increased or not. On the other hand, in the case of ROMK, we did not find differences in ROMK expression in the kidney between wild-type and KLHL3$^{R528H/+}$ mice. However, we were unable to perform microdissection of kidney, and the available anti-ROMK antibody detects all ROMK variants. Therefore, to clarify the *in vivo* effect of KLHL3 on ROMK in CCD, further investigation is required.

In summary, we established and analyzed KLHL3$^{R528H/+}$ knock-in mice, and clarified the essential pathogenesis of mutant KLHL3-induced PHAII. Mutant KLHL3 causes accumulation of both WNK1 and WNK4 at DCT due to loss of binding ability of KLHL3 to WNK kinases. This regulation of the WNK-OSR1/SPAK-NCC phosphorylation cascade by Cullin3-KLHL3 E3 ligase complexes plays important physiological and pathophysiological roles for sodium handling in the kidney *in vivo*.

MATERIALS AND METHODS

Generation of KLHL3$^{R528H/+}$ knock-in mice

To generate KLHL3$^{R528/+}$ knock-in mice, the targeting vector was prepared using the BAC recombineering system (40). The point mutation (R528H) was introduced into exon 15 of the targeting vector by *galK* selection system (41). The targeting vector was then transfected into Baltha1 ES cells (25), which are derived from C57BL/6 mice, by electroporation as previously reported (42). After selection with 150 μg/ml G418 and 2 μM ganciclovir, targeted ES clones were selected by PCR with a sense primer F1 (5′-ATA GCA GAG CCG TCT CTG TG-3′) located within the neo cassette and an antisense primer R1 (5′-ACT TGT GTA GCG CCA AGT GC-3′) located following exon 15, Southern blotting and sequencing of the mutation site. Selected ES clones were injected into C57BL/6 morula. Chimeric males were bred with C57BL/6 females to produce mutant KLHL3$^{flox/+}$ (R528H) mice, and the neo cassette was then deleted by crossing these mutant KLHL3$^{flox/+}$ mice with transgenic mice expressing Cre recombinase under the control of the CAG promoter (43). Offsprings were genotyped by PCR with sense primer F2 (5′-CAC AGG GTA ACT GGG GCT GGT-3′) and antisense primer R2 (5′-GGA AGA ACT GTG ACC CCC GC-3′) flanking the remaining loxP site and exon 15.

Animals

Studies were performed using 10-week-old mice that had free access to food and water. Mice of each genotype were placed on a normal-salt diet (NaCl 0.4% w/w) or a high-salt diet (8.0% w/w) for 1 week. All experiments were performed 1 week after dietary change. The Animal Care and Use Committee of Tokyo Medical and Dental University approved the experimental protocol.

Measurement of blood pressure

We measured blood pressure by using a radiotelemetric method in which a blood pressure transducer (Data Sciences International, St. Paul, MN, USA) was inserted into the left carotid artery. Seven days after transplantation, each mouse was housed individually in a standard cage on a receiver under a 12 h light–dark cycle. Systolic and diastolic blood pressure was recorded every minute via radiotelemetry. For each mouse, we measured blood pressure values for more than 3 consecutive days and calculated the mean ± SE of all values. These experiments were performed under a normal-salt (NaCl 0.4% w/w) or high-salt (8.0% w/w) diet.

Blood analysis

Blood was drawn from the retro-orbital sinus under light ether anesthesia. Serum data were determined using the i-STAT system (FUSO Pharmaceutical Industries, Osaka, Japan).

Immunoblot analysis

Immunoblot analyses were performed on kidney homogenates. Kidneys were dissected from mice. Homogenates of whole kidney without the nuclear fraction (600 g) were prepared, and the crude membrane fraction (17 000 g) was used to measure the levels of NCC as described previously (7). Blots were probed with the following primary antibodies: anti-WNK1 (A301–516A; Bethyl, Montgomery, TX, USA), anti-WNK4 (36), anti-total OSR1 (M10; Abnova, Taipei, Taiwan), anti-phosphorylated OSR1 (44), anti-total SPAK (Cell Signaling Technology, Danvers, MA, USA), anti-phosphorylated SPAK (33), anti-total NCC (29), anti-phosphorylated NCC (pSer71) (28), anti-ENaC α subunit (kindly provided by M. Knepper), anti-ENaC β subunit (Alomone, Jerusalem, Israel), anti-ENaC γ subunit (kindly provided by M. Knepper), and anti-ROMK antibodies (kindly provided by J. B. Wade and P. A. Welling) (45), anti-actin (Cytoskeleton, Denver, CO, USA). Alkaline-phosphatase-conjugated anti-IgG antibodies (Promega, Madison, WI, USA) and Western Blue (Promega) were used to detect the signals. The relative intensities of immunoblot bands were determined by densitometry with YabGelImage free software.

Quantitative PCR analysis

Quantitative PCR analysis was performed on kidney as previously described (46). Total RNA from mouse kidneys was extracted using TRIzol reagent (Invitrogen, Carlsbad, CA, USA), according to the manufacturer's instructions. Total RNA was reverse transcribed using Omniscript reverse transcriptase (Qiagen, Hilden, Germany). Quantitative real-time PCR by Thermal Cycler Dice (Takara Bio, Otsu, Japan) was performed using the primer sets shown in a previous report (47).

Immunofluorescence

Kidneys were fixed by perfusion with periodate lysine (0.2 M) and paraformaldehyde (2%) in PBS. Immunofluorescence was performed as previously described (42). The primary antibodies used were anti-KLHL3 (Proteintech, Chicago, IL, USA), anti-WNK1 (A301–516A; BETHYL), anti-WNK4 (36), anti-NCC (29) and anti-pNCC (pSer71) (28). Alexa 488 or 546 dye-labeled (Molecular Probes; Invitrogen) secondary antibodies were used for immunofluorescence. Immunofluorescence images were obtained using an LSM510 Meta Confocal Microscope (Carl Zeiss, Oberkochen, Germany).

Fluorescence correlation spectroscopy

Fluorescent TAMRA-labeled WNK1 and WNK4 peptides covering the acidic motif were prepared (Hokkaido System Science Co., Ltd., Hokkaido, Japan). Human full-length KLHL3 (wild-type and R528H mutant) was cloned into pGEX6P-1 vectors. The recombinant GST-fusion KLHL3 protein expressed in BL21 *Escherichia coli* cells was purified using glutathione Sepharose beads. The TAMRA-labeled WNK peptides were incubated at room temperature for 30 min with different concentrations of GST-KLHL3 (0–2 μM) in 1× PBS containing 0.05% Tween 20 (reaction buffer). FCS measurements using the FluoroPoint-light analytical system (Olympus, Tokyo, Japan) were performed as previously described (26,27). The measurements were repeated five times per sample.

Statistics

Data are presented as means ± SE. A student's *t*-test was used for comparisons between groups. ANOVA and Tukey's test were used for multiple comparisons.

SUPPLEMENTARY MATERIAL

Supplementary Material is available at *HMG* online.

ACKNOWLEDGEMENTS

We thank C. Iijima for help in the experiments. We thank M. Knepper, J. B. Wade and P. A. Welling for provision of antibodies.

Conflict of Interest statement. The authors declare that they have no conflict of interest.

FUNDING

This study was supported, in part, by Grants-in-Aid for Scientific Research (S, A) from the Japan Society for the Promotion of Science; Grant-in-Aid for Young Scientists (B) from the Ministry of Education, Culture, Sports, Science and Technology of Japan; a Health and Labor Sciences Research Grant from the Ministry of Health, Labor and Welfare; the Salt Science Research Foundation (grant no. 1228); the Takeda Science Foundation; Banyu Foundation Research Grant and the Vehicle Racing Commemorative Foundation.

REFERENCES

1. Gordon, R.D. (1986) Syndrome of hypertension and hyperkalemia with normal glomerular filtration rate. *Hypertension*, **8**, 93–102.
2. Achard, J.M., Disse-Nicodeme, S., Fiquet-Kempf, B. and Jeunemaitre, X. (2001) Phenotypic and genetic heterogeneity of familial hyperkalaemic hypertension (Gordon syndrome). *Clin. Exp. Pharmacol. Physiol.*, **28**, 1048–1052.
3. Wilson, F.H., Disse-Nicodème, S., Choate, K.A., Ishikawa, K., Nelson-Williams, C., Desitter, I., Gunel, M., Milford, D.V., Lipkin, G.W., Achard, J.M. *et al.* (2001) Human hypertension caused by mutations in WNK kinases. *Science*, **293**, 1107–1112.
4. Moriguchi, T., Urushiyama, S., Hisamoto, N., Iemura, S., Uchida, S., Natsume, T., Matsumoto, K. and Shibuya, H. (2005) WNK1 regulates phosphorylation of cation-chloride-coupled cotransporters via the STE20-related kinases, SPAK and OSR1. *J. Biol. Chem.*, **280**, 42685–42693.
5. Vitari, A.C., Deak, M., Morrice, N.A. and Alessi, D.R. (2005) The WNK1 and WNK4 protein kinases that are mutated in Gordon's hypertension syndrome phosphorylate and activate SPAK and OSR1 protein kinases. *Biochem. J.*, **391**, 17–24.
6. Chiga, M., Rafiqi, F.H., Alessi, D.R., Sohara, E., Ohta, A., Rai, T., Sasaki, S. and Uchida, S. (2011) Phenotypes of pseudohypoaldosteronism type II caused by the WNK4 D561A missense mutation are dependent on the WNK-OSR1/SPAK kinase cascade. *J. Cell. Sci.*, **124**, 1391–1395.
7. Yang, S.S., Morimoto, T., Rai, T., Chiga, M., Sohara, E., Ohno, M., Uchida, K., Lin, S.H., Moriguchi, T., Shibuya, H. *et al.* (2007) Molecular pathogenesis of pseudohypoaldosteronism type II: generation and analysis of a Wnk4(D561A/+) knockin mouse model. *Cell. Metab.*, **5**, 331–344.
8. Bergaya, S., Faure, S., Baudrie, V., Rio, M., Escoubet, B., Bonnin, P., Henrion, D., Loirand, G., Achard, J.M., Jeunemaitre, X. *et al.* (2011) WNK1 regulates vasoconstriction and blood pressure response to {alpha}1-adrenergic stimulation in mice. *Hypertension*, **58**, 439–445.
9. Vidal-Petiot, E., Elvira-Matelot, E., Mutig, K., Soukaseum, C., Baudrie, V., Wu, S., Cheval, L., Huc, E., Cambillau, M., Bachmann, S. *et al.* (2013) WNK1-related familial hyperkalemic hypertension results from an increased expression of L-WNK1 specifically in the distal nephron. *Proc. Natl Acad. Sci. USA*, **110**, 14366–14371.
10. Castañeda-Bueno, M., Cervantes-Pérez, L.G., Vázquez, N., Uribe, N., Kantesaria, S., Morla, L., Bobadilla, N.A., Doucet, A., Alessi, D.R. and Gamba, G. (2012) Activation of the renal Na+:Cl- cotransporter by angiotensin II is a WNK4-dependent process. *Proc. Natl Acad. Sci. USA*, **109**, 7929–7934.
11. Rafiqi, F.H., Zuber, A.M., Glover, M., Richardson, C., Fleming, S., Jovanović, S., Jovanović, A., O'Shaughnessy, K.M. and Alessi, D.R. (2010) Role of the WNK-activated SPAK kinase in regulating blood pressure. *EMBO Mol. Med.*, **2**, 63–75.
12. Yang, S.S., Lo, Y.F., Wu, C.C., Lin, S.W., Yeh, C.J., Chu, P., Sytwu, H.K., Uchida, S., Sasaki, S. and Lin, S.H. (2010) SPAK-knockout mice manifest Gitelman syndrome and impaired vasoconstriction. *J. Am. Soc. Nephrol.*, **21**, 1868–1877.
13. Lin, S.H., Yu, I.S., Jiang, S.T., Lin, S.W., Chu, P., Chen, A., Sytwu, H.K., Sohara, E., Uchida, S., Sasaki, S. *et al.* (2011) Impaired phosphorylation of Na(+)-K(+)-2Cl(-) cotransporter by oxidative stress-responsive kinase-1 deficiency manifests hypotension and Bartter-like syndrome. *Proc. Natl Acad. Sci. USA*, **108**, 17538–17543.
14. Susa, K., Kita, S., Iwamoto, T., Yang, S.S., Lin, S.H., Ohta, A., Sohara, E., Rai, T., Sasaki, S., Alessi, D.R. *et al.* (2012) Effect of heterozygous deletion of WNK1 on the WNK-OSR1/ SPAK-NCC/NKCC1/NKCC2 signal cascade in the kidney and blood vessels. *Clin. Exp. Nephrol.*, **16**, 530–538.
15. Boyden, L.M., Choi, M., Choate, K.A., Nelson-Williams, C.J., Farhi, A., Toka, H.R., Tikhonova, I.R., Bjornson, R., Mane, S.M., Colussi, G. *et al.* (2012) Mutations in kelch-like 3 and cullin 3 cause hypertension and electrolyte abnormalities. *Nature*, **482**, 98–102.
16. Louis-Dit-Picard, H., Barc, J., Trujillano, D., Miserey-Lenkei, S., Bouatia-Naji, N., Pylypenko, O., Beaurain, G., Bonnefond, A., Sand, O., Simian, C. *et al.* (2012) KLHL3 mutations cause familial hyperkalemic hypertension by impairing ion transport in the distal nephron. *Nat. Genet.*, **44**, 456–460, 456–460.
17. Kigoshi, Y., Tsuruta, F. and Chiba, T. (2011) Ubiquitin ligase activity of Cul3-KLHL7 protein is attenuated by autosomal dominant retinitis pigmentosa causative mutation. *J. Biol. Chem.*, **286**, 33613–33621.

18. Lee, Y.R., Yuan, W.C., Ho, H.C., Chen, C.H., Shih, H.M. and Chen, R.H. (2010) The Cullin 3 substrate adaptor KLHL20 mediates DAPK ubiquitination to control interferon responses. *EMBO J.*, **29**, 1748–1761.
19. Lin, M.Y., Lin, Y.M., Kao, T.C., Chuang, H.H. and Chen, R.H. (2011) PDZ-RhoGEF ubiquitination by Cullin3-KLHL20 controls neurotrophin-induced neurite outgrowth. *J. Cell Biol.*, **193**, 985–994.
20. Uchida, S., Sohara, E., Rai, T. and Sasaki, S. (2013) Regulation of with-no-lysine kinase signaling by Kelch-like proteins. *Biol. Cell*, **106**, 45–56.
21. Wakabayashi, M., Mori, T., Isobe, K., Sohara, E., Susa, K., Araki, Y., Chiga, M., Kikuchi, E., Nomura, N., Mori, Y. *et al.* (2013) Impaired KLHL3-mediated ubiquitination of WNK4 causes human hypertension. *Cell Rep.*, **3**, 858–868.
22. Wu, G. and Peng, J.B. (2013) Disease-causing mutations in KLHL3 impair its effect on WNK4 degradation. *FEBS Lett.*, **587**, 1717–1722.
23. Shibata, S., Zhang, J., Puthumana, J., Stone, K.L. and Lifton, R.P. (2013) Kelch-like 3 and Cullin 3 regulate electrolyte homeostasis via ubiquitination and degradation of WNK4. *Proc. Natl Acad. Sci. USA*, **110**, 7838–7843.
24. Ohta, A., Schumacher, F.R., Mehellou, Y., Johnson, C., Knebel, A., Macartney, T.J., Wood, N.T., Alessi, D.R. and Kurz, T. (2013) The CUL3-KLHL3 E3 ligase complex mutated in Gordon's hypertension syndrome interacts with and ubiquitylates WNK isoforms: disease-causing mutations in KLHL3 and WNK4 disrupt interaction. *Biochem. J.*, **451**, 111–122.
25. Kim-Kaneyama, J.R., Takeda, N., Sasai, A., Miyazaki, A., Sata, M., Hirabayashi, T., Shibanuma, M., Yamada, G. and Nose, K. (2011) Hic-5 deficiency enhances mechanosensitive apoptosis and modulates vascular remodeling. *J. Mol. Cell. Cardiol.*, **50**, 77–86.
26. Mori, Y., Wakabayashi, M., Mori, T., Araki, Y., Sohara, E., Rai, T., Sasaki, S. and Uchida, S. (2013) Decrease of WNK4 ubiquitination by disease-causing mutations of KLHL3 through different molecular mechanisms. *Biochem. Biophys. Res. Commun.*, **439**, 30–34.
27. Takahashi, D., Mori, T., Wakabayashi, M., Mori, Y., Susa, K., Zeniya, M., Sohara, E., Rai, T., Sasaki, S. and Uchida, S. (2013) KLHL2 interacts with and ubiquitinates WNK kinases. *Biochem. Biophys. Res. Commun.*, **437**, 457–462.
28. Sohara, E., Rai, T., Yang, S.S., Ohta, A., Naito, S., Chiga, M., Nomura, N., Lin, S.H., Vandewalle, A., Ohta, E. *et al.* (2011) Acute insulin stimulation induces phosphorylation of the Na-Cl cotransporter in cultured distal mpkDCT cells and mouse kidney. *PLoS One*, **6**, e24277.
29. Nishida, H., Sohara, E., Nomura, N., Chiga, M., Alessi, D.R., Rai, T., Sasaki, S. and Uchida, S. (2012) Phosphatidylinositol 3-kinase/Akt signaling pathway activates the WNK-OSR1/SPAK-NCC phosphorylation cascade in hyperinsulinemic db/db mice. *Hypertension*, **60**, 981–990.
30. Chávez-Canales, M., Arroyo, J.P., Ko, B., Vázquez, N., Bautista, R., Castañeda-Bueno, M., Bobadilla, N.A., Hoover, R.S. and Gamba, G. (2013) Insulin increases the functional activity of the renal NaCl cotransporter. *J. Hypertens.*, **31**, 303–311.
31. Komers, R., Rogers, S., Oyama, T.T., Xu, B., Yang, C.L., McCormick, J. and Ellison, D.H. (2012) Enhanced phosphorylation of Na(+)-Cl- co-transporter in experimental metabolic syndrome: role of insulin. *Clin. Sci. (Lond.)*, **123**, 635–647.
32. Talati, G., Ohta, A., Rai, T., Sohara, E., Naito, S., Vandewalle, A., Sasaki, S. and Uchida, S. (2010) Effect of angiotensin II on the WNK-OSR1/SPAK-NCC phosphorylation cascade in cultured mpkDCT cells and in vivo mouse kidney. *Biochem. Biophys. Res. Commun.*, **393**, 844–848.
33. Zeniya, M., Sohara, E., Kita, S., Iwamoto, T., Susa, K., Mori, T., Oi, K., Chiga, M., Takahashi, D., Yang, S.S. *et al.* (2013) Dietary salt intake regulates WNK3-SPAK-NKCC1 phosphorylation cascade in mouse aorta through angiotensin II. *Hypertension*, **62**, 872–878.
34. San-Cristobal, P., Pacheco-Alvarez, D., Richardson, C., Ring, A.M., Vazquez, N., Rafiqi, F.H., Chari, D., Kahle, K.T., Leng, Q., Bobadilla, N.A. *et al.* (2009) Angiotensin II signaling increases activity of the renal Na-Cl cotransporter through a WNK4-SPAK-dependent pathway. *Proc. Natl Acad. Sci. USA*, **106**, 4384–4389.
35. Chiga, M., Rai, T., Yang, S.S., Ohta, A., Takizawa, T., Sasaki, S. and Uchida, S. (2008) Dietary salt regulates the phosphorylation of OSR1/SPAK kinases and the sodium chloride cotransporter through aldosterone. *Kidney Int.*, **74**, 1403–1409.
36. Susa, K., Sohara, E., Isobe, K., Chiga, M., Rai, T., Sasaki, S. and Uchida, S. (2012) WNK-OSR1/SPAK-NCC signal cascade has circadian rhythm dependent on aldosterone. *Biochem. Biophys. Res. Commun.*, **427**, 743–747.
37. Rozansky, D.J., Cornwall, T., Subramanya, A.R., Rogers, S., Yang, Y.F., David, L.L., Zhu, X., Yang, C.L. and Ellison, D.H. (2009) Aldosterone mediates activation of the thiazide-sensitive Na-Cl cotransporter through an SGK1 and WNK4 signaling pathway. *J. Clin. Invest.*, **119**, 2601–2612.
38. McCormick, J.A., Nelson, J.H., Yang, C.L., Curry, J.N. and Ellison, D.H. (2011) Overexpression of the sodium chloride cotransporter is not sufficient to cause familial hyperkalemic hypertension. *Hypertension*, **58**, 888–894.
39. Wang, Q., Hummler, E., Nussberger, J., Clément, S., Gabbiani, G., Brunner, H.R. and Burnier, M. (2002) Blood pressure, cardiac, and renal responses to salt and deoxycorticosterone acetate in mice: role of Renin genes. *J. Am. Soc. Nephrol.*, **13**, 1509–1516.
40. Liu, P., Jenkins, N.A. and Copeland, N.G. (2003) A highly efficient recombineering-based method for generating conditional knockout mutations. *Genome Res.*, **13**, 476–484.
41. Warming, S., Costantino, N., Court, D.L., Jenkins, N.A. and Copeland, N.G. (2005) Simple and highly efficient BAC recombineering using galK selection. *Nucleic Acids Res.*, **33**, e36.
42. Sohara, E., Rai, T., Yang, S.S., Uchida, K., Nitta, K., Horita, S., Ohno, M., Harada, A., Sasaki, S. and Uchida, S. (2006) Pathogenesis and treatment of autosomal-dominant nephrogenic diabetes insipidus caused by an aquaporin 2 mutation. *Proc. Natl Acad. Sci. USA*, **103**, 14217–14222.
43. Sakai, K. and Miyazaki, J. (1997) A transgenic mouse line that retains Cre recombinase activity in mature oocytes irrespective of the cre transgene transmission. *Biochem. Biophys. Res. Commun.*, **237**, 318–324.
44. Ohta, A., Rai, T., Yui, N., Chiga, M., Yang, S.S., Lin, S.H., Sohara, E., Sasaki, S. and Uchida, S. (2009) Targeted disruption of the Wnk4 gene decreases phosphorylation of Na-Cl cotransporter, increases Na excretion and lowers blood pressure. *Hum. Mol. Genet.*, **18**, 3978–3986.
45. Wade, J.B., Fang, L., Coleman, R.A., Liu, J., Grimm, P.R., Wang, T. and Welling, P.A. (2011) Differential regulation of ROMK (Kir1.1) in distal nephron segments by dietary potassium. *Am. J. Physiol. Renal. Physiol.*, **300**, F1385–F1393.
46. Oi, K., Sohara, E., Rai, T., Misawa, M., Chiga, M., Alessi, D.R., Sasaki, S. and Uchida, S. (2012) A minor role of WNK3 in regulating phosphorylation of renal NKCC2 and NCC co-transporters in vivo. *Biol. Open*, **1**, 120–127.
47. O'Reilly, M., Marshall, E., Macgillivray, T., Mittal, M., Xue, W., Kenyon, C.J. and Brown, R.W. (2006) Dietary electrolyte-driven responses in the renal WNK kinase pathway in vivo. *J. Am. Soc. Nephrol.*, **17**, 2402–2413.